

NASA Technical Memorandum 107745

IN-02  
158550  
p. 29

**HIGH-ORDER "CYCLO-DIFFERENCE" TECHNIQUES:  
AN ALTERNATIVE TO FINITE DIFFERENCES**

**Mark H. Carpenter and John C. Otto**

**MARCH 1993**

(NASA-TM-107745) HIGH-ORDER  
CYCLO-DIFFERENCE TECHNIQUES: AN  
ALTERNATIVE TO FINITE DIFFERENCES  
(NASA) 29 p

N93-25074

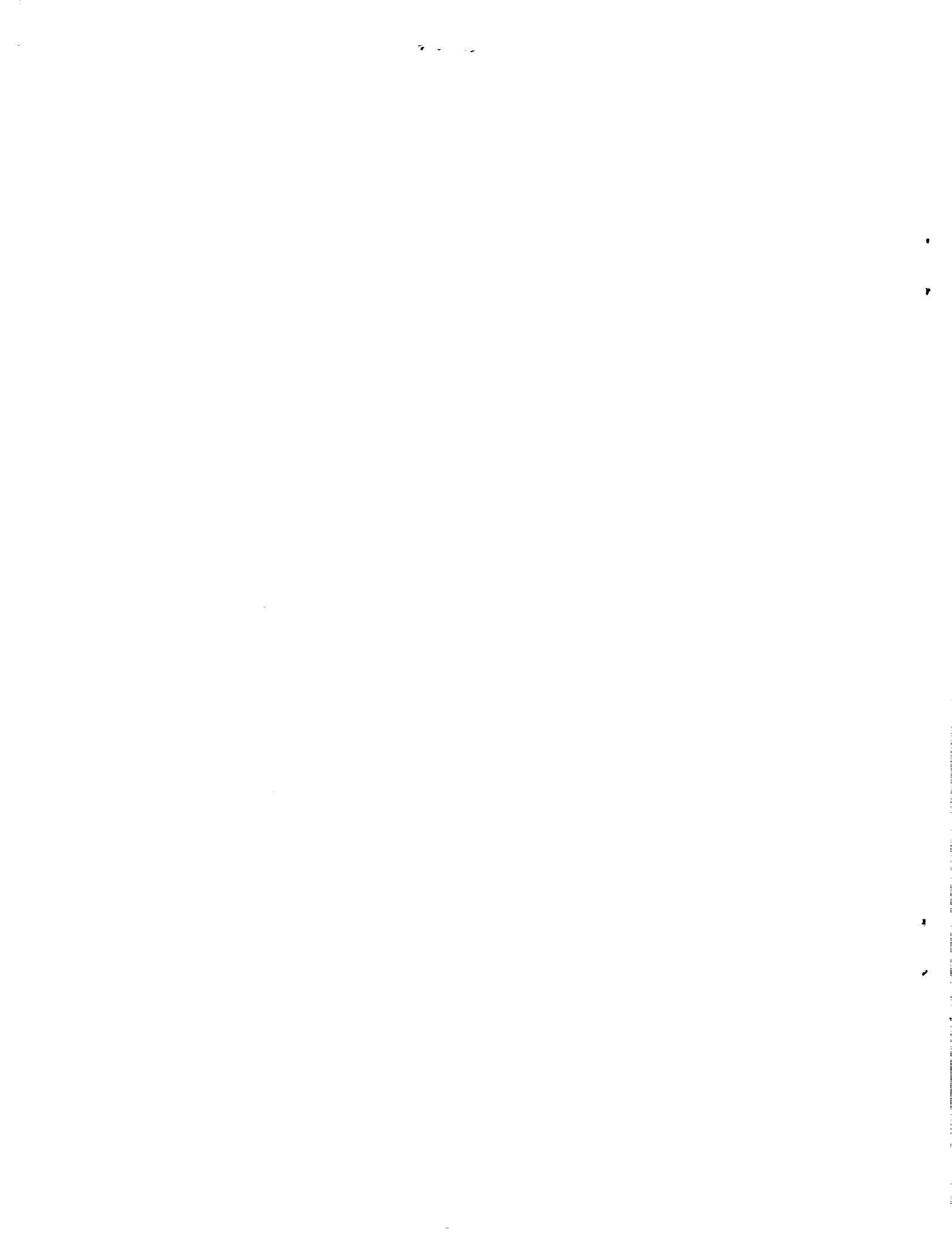
Unclass

G3/02 0158550



National Aeronautics and  
Space Administration

**Langley Research Center**  
Hampton, Virginia 23681-0001



# HIGH-ORDER "CYCLO-DIFFERENCE" TECHNIQUES: AN ALTERNATIVE TO FINITE DIFFERENCES

Mark H. Carpenter \* and John Otto †

## ABSTRACT

The summation-by-parts energy norm is used to establish a new class of high-order finite-difference techniques referred to here as "cyclo-difference" techniques. These techniques are constructed cyclically from stable subelements, and require no numerical boundary conditions; when coupled with the simultaneous approximation term (SAT) boundary treatment, they are time asymptotically stable for an arbitrary hyperbolic system. These techniques are similar to spectral element techniques and are ideally suited for parallel implementation, but do not require special collocation points or orthogonal basis functions. The principal focus of this work is on methods of sixth-order formal accuracy or less; however, these methods could be extended in principle to any arbitrary order of accuracy.

## INTRODUCTION

A great deal of effort has recently been placed on high-order finite-difference techniques (both central and upwind) for direct numerical simulations. A significant problem that faces the high-order finite-difference community is the closure of those boundary schemes that retain the formal accuracy of the underlying method and do not cause instability. To retain the  $N$ th-order formal accuracy of the interior scheme for an arbitrary hyperbolic equation, the numerical boundaries must be closed with an accuracy of no less than  $(N - 1)$ th order [1]. Such closures often cause numerical instability and cannot be used. (e.g., [2]). Recently, a precise means of determining boundary closures that maintain both stability and accuracy has been developed based on the summation-by-parts energy norm. (See references [3], [4], and [5].) A numerical discretization that satisfies specific criteria on the discretization matrix  $A^*$  automatically satisfies a discrete energy norm. Central-difference schemes

---

\*Research Scientist, Theoretical Flow Physics Branch, Fluid Mechanics Division, NASA Langley Research Center, Hampton, VA.

†Research Scientist, Computational Sciences Branch, Fluid Mechanics Division, NASA Langley Research Center, Hampton, VA.

automatically satisfy these properties in their interior. The task is, therefore, to find high-order closure techniques at the boundaries that maintain the specific form of the matrix  $A^*$ . This can be a daunting task, but can be accomplished [2], [4], [5].

One of the advantages of spectral techniques is that the ambiguity of numerical boundary treatments is not present. The global nature of the method relies on a specific stencil at each point. Each individual point may be unstable, but the scheme as a whole is stable and accurate. This notion motivates us to develop a new class of finite-difference schemes. Like central-difference and spectral techniques, they are not biased in the direction of a physical eigenvalue and, therefore, do not require eigenvalue decomposition when used for general hyperbolic equations. Unlike central-difference techniques, each point has its own specific stencil. Although individual stencils may appear to be unstable locally, the global method is stable and accurate. Taylor series analysis guarantees that each point has a local order property. The use of a specific energy norm to derive the stencils guarantees that the resulting global scheme will be stable.

Another problem with high-order finite-difference techniques, as well as spectral single-domain techniques, is their implementation on parallel machines. For conventional finite-difference techniques (central or upwind difference), as the order of accuracy increases, the stencil width also increases. This results in increased overhead in communicating between processors. Spectral element techniques are both efficient and accurate methods for implementation on parallel machines [6]. The problem is divided into several domains, and each domain is assigned to a processor. Only one point of the stencil coexists on multiple processors in spectral element techniques. Information transfer between processors is kept to a minimum under these circumstances.

Cyclo-difference techniques are a combination of high-order finite-difference techniques and spectral element techniques. They rely on an existing energy-norm proof to establish their stability for the hyperbolic system and require no special boundary closure stencils. These techniques can easily be split on multi-processor environments. This flexibility results because the discretizations are composed of many subelements that each satisfy an order and stability property. The subelements are then patched together recursively such that the resulting scheme retains the same stability properties. For parallel implementation, they can easily be broken at the patch location, which results in a minimum of communication for an arbitrarily high-order scheme.

## SUMMATION-BY-PARTS ENERGY NORM

### Stability of Continuous System

As shown in reference [5], the summation-by-parts energy norm mimics, at the semidiscrete level, the continuous behavior of the principle of the conservation of energy. Because the entire foundation

of the cyclo-difference methodology is based on this norm, a complete derivation of the conservation of energy principle in the continuous and the discrete case is presented. The model problem is the hyperbolic equation defined by

$$\frac{\partial U}{\partial t} + \frac{\partial U}{\partial x} = 0 \quad 0 \leq x \leq 1, t \geq 0 \quad (1)$$

$$U(0, t) = f(t) \quad t \geq 0 \quad (2)$$

$$U(x, 0) = \psi(x) \quad 0 \leq x \leq 1 \quad (3)$$

We begin by defining an energy as  $E(t) = U^2$ ,  $t > 0$ . If the energy is differentiated with respect to time and the values of  $U_t$  from equation (1) are substituted, then integration over the domain yields

$$E_t(t) = \int_0^1 \left[ -\frac{\partial(U^2)}{\partial x} \right] \quad t \geq 0 \quad (4)$$

The definite integral in equation (4) is performed to yield

$$E_t(t) = -[U^2(1, t) - U^2(0, t)] \quad (5)$$

and the boundary conditions are substituted from equation (2) to yield

$$E_t(t) = -[U^2(1, t) - f^2(t)] \quad (6)$$

If certain properties on the boundary condition  $f(t)$  are assumed, the equation is dissipative (decays energy) for all time. For example, if  $f(t) = 0$ , then the system energy is uniformly dissipative.

### Stability of Discrete System

Discrete spatial operators that satisfy very specific properties are shown to be stable in a manner analogous to that used in the previous proof of stability. These operators satisfy the summation-by-parts energy norm. For example, given the scalar hyperbolic equation  $U_t + U_x = 0$ , a general semidiscretization can be written as  $U_t + A^*U = 0$ , where  $A^*$  is the spatial discretization matrix that is presumably consistent to some order. This matrix  $A^*$  can, in general, be decomposed into the form

$$A^* = P^{-1} Q \quad (7)$$

This decomposition is in general not unique. If a decomposition can be found such that

1. Symmetric  $P$  : ( $P = P^T$ ) ( $p_{i,j} = p_{j,i}$ )
2. Positive definite  $P$  : ( $W^T P W > 0$ )

3. Nearly skew-symmetric  $Q$  :  $(q_{i,j} = -q_{j,i} + 2\delta_{i,1} \delta_{1,j} q_{1,1} + 2\delta_{i,N} \delta_{N,j} q_{N,N})$

4.  $q_{N,N} > 0$  and  $q_{1,1} = -q_{N,N}$

then the discretization matrix  $A^*$  automatically satisfies the summation-by-parts energy norm. (See reference [5].)

To illustrate that this stability property results directly from the form of the matrices  $P$  and  $Q$ , a proof is presented for the semidiscrete form defined by equations (1) and (2). Note that the spatial discretization operator can be written in the form

$$P U_x = Q U; \quad U_x = P^{-1} Q U \quad (8)$$

where  $P^{-1}$  exists and  $U$  is the vector of discrete values  $(U_1, U_2, U_3, \dots, U_{N-2}, U_{N-1}, U_N)^T$ . The semidiscrete version of equation (1) becomes

$$P \frac{\partial U}{\partial t} + Q U = 0 \quad t \geq 0 \quad (9)$$

We define the discrete energy as

$$E(t) = (U^T P U) \quad t \geq 0 \quad (10)$$

where  $P$  must be positive definite to ensure that  $E(t)$  is a strictly positive number. Equation (10) is differentiated with respect to time to yield the expression

$$E_t(t) = \left[ \frac{\partial U^T}{\partial t} P U + U^T P \frac{\partial U}{\partial t} \right] \quad t \geq 0 \quad (11)$$

Because  $P$  is symmetric ( $P = P^T$ ), equation (11) becomes

$$E_t(t) = 2 \left[ U^T P \frac{\partial U}{\partial t} \right] \quad t \geq 0 \quad (12)$$

The semidiscrete expression [equation (9)] is substituted into equation (12) to yield

$$E_t(t) = 2 [-U^T Q U] \quad t \geq 0 \quad (13)$$

By using the matrix  $Q$  and the relationship between the values  $q_{0,0}$  and  $q_{N,N}$ , one obtains an energy of the form

$$E_t(t) = -2 q_{N,N} [U_N^2 - U_0^2] \quad (14)$$

The boundary condition defined in equation (2) is substituted to yield

$$E_t(t) = -2 q_{N,N} [U_N^2 - f^2(t)] \quad (15)$$

Note that the time rate of change of the discrete energy defined in equation (15) is identical in form (to within a positive constant) to that of the continuous case equation (5).

## CYCLO-DIFFERENCING

Conventional central- and upwind-difference techniques use one stencil for the inner portion of the spatial domain and auxiliary formulas at the boundaries such that the resulting scheme is stable. Spectral element techniques use orthogonal basis functions to define local elements and then connect them with various methods that range from spectral patching to flux balances [7]. The simplicity and stability of the cyclo-differencing relies on a very specific property of the summation-by-parts energy norm. Assume for a particular set of discrete points  $x_j$ ,  $j = 1, N$  that a stable discretization has been isolated that satisfies all criteria of the summation-by-parts energy norm. The resulting semidiscretization written in matrix form is  $P \vec{U}_t = Q \vec{U}$ , where

$$P = \begin{bmatrix} p_{1,1} & p_{1,2} & \cdot & \cdot & \cdot & p_{1,N-1} & p_{1,N} \\ p_{1,2} & p_{2,2} & \cdot & \cdot & \cdot & p_{2,N-1} & p_{2,N} \\ \cdot & \cdot & & & & \cdot & \cdot \\ \cdot & \cdot & & & & \cdot & \cdot \\ p_{1,N-1} & p_{1,N-2} & \cdot & \cdot & \cdot & p_{N-1,N-1} & p_{N-1,N} \\ p_{1,N} & p_{2,N} & \cdot & \cdot & \cdot & p_{N-1,N} & p_{N,N} \end{bmatrix}; \quad \vec{U}_t = \begin{bmatrix} \partial U_1 / \partial t \\ \partial U_2 / \partial t \\ \vdots \\ \partial U_{N-1} / \partial t \\ \partial U_N / \partial t \end{bmatrix};$$

$$Q = \frac{1}{\Delta} \begin{bmatrix} -q_{N,N} & q_{1,2} & \cdot & \cdot & \cdot & q_{1,N-1} & q_{1,N} \\ -q_{1,2} & 0 & \cdot & \cdot & \cdot & q_{2,N-1} & q_{2,N} \\ \cdot & \cdot & & & & \cdot & \cdot \\ \cdot & \cdot & & & & \cdot & \cdot \\ \cdot & \cdot & & & & \cdot & \cdot \\ -q_{1,N-1} & -q_{1,N-2} & \cdot & \cdot & \cdot & 0 & q_{N-1,N} \\ -q_{1,N} & -q_{2,N} & \cdot & \cdot & \cdot & -q_{N-1,N} & q_{N,N} \end{bmatrix}; \quad \vec{U} = \begin{bmatrix} U_1 \\ U_2 \\ \vdots \\ U_{N-1} \\ U_N \end{bmatrix}$$

Note that  $P$  is symmetric (and positive definite) and  $Q$  is skew symmetric except for the elements  $q_{1,1}$  and  $q_{N,N}$ , where  $q_{1,1} = -q_{N,N}$ . Also note that the grid-spacing  $\Delta$  has been factored out of the matrix  $Q$ . No attempt has been made to specify the value of the constant  $N$ . A cyclo-difference scheme is constructed by recursively patching the stable base schemes together, which is illustrated by the following example. Assume that the discretization involved  $2N - 1$  uniformly distributed points instead of  $N$  points. We can use the properties of the matrices  $P$  and  $Q$  (of dimension  $N$ ) to define a discretization over the  $2N - 1$  points that satisfies all criteria of the summation-by-parts energy norm, and is therefore stable for any system of hyperbolic equations. We define this new semidiscretization on the equation  $U_t + U_x = 0$  as  $\hat{P} \vec{U}_t = \hat{Q} \vec{U}$  and construct it as

$$\hat{P} = \begin{bmatrix} p_{1,1} & p_{1,2} & \dots & p_{1,N-1} & p_{1,N} & 0 & \dots & 0 & 0 \\ p_{1,2} & p_{2,2} & \dots & p_{2,N-1} & p_{2,N} & 0 & \dots & 0 & 0 \\ \vdots & \vdots & & \vdots & \vdots & 0 & \dots & 0 & 0 \\ \vdots & \vdots & & \vdots & \vdots & 0 & \dots & 0 & 0 \\ \vdots & \vdots & & \vdots & \vdots & 0 & \dots & 0 & 0 \\ p_{1,N-1} & p_{1,N-2} & \dots & p_{N-1,N-1} & p_{N-1,N} & 0 & \dots & 0 & 0 \\ p_{1,N} & p_{2,N} & \dots & p_{N-1,N} & p_{N,N} + p_{1,1} & p_{1,2} & \dots & p_{1,N-1} & p_{1,N} \\ 0 & 0 & \dots & 0 & p_{1,2} & p_{2,2} & \dots & p_{2,N-1} & p_{2,N} \\ 0 & 0 & \dots & 0 & \vdots & \vdots & \dots & \vdots & \vdots \\ 0 & 0 & \dots & 0 & \vdots & \vdots & \dots & \vdots & \vdots \\ 0 & 0 & \dots & 0 & \vdots & \vdots & \dots & \vdots & \vdots \\ 0 & 0 & \dots & 0 & p_{1,N-1} & p_{1,N-2} & \dots & p_{N-1,N-1} & p_{N-1,N} \\ 0 & 0 & \dots & 0 & p_{1,N} & p_{2,N} & \dots & p_{N-1,N} & p_{N,N} \end{bmatrix} ;$$

$$\hat{Q} = \frac{1}{\Delta} \begin{bmatrix} -q_{N,N} & q_{1,2} & \dots & q_{1,N-1} & q_{1,N} & 0 & \dots & 0 & 0 \\ -q_{1,2} & 0 & \dots & q_{2,N-1} & q_{2,N} & 0 & \dots & 0 & 0 \\ \vdots & \vdots & & \vdots & \vdots & 0 & \dots & 0 & 0 \\ \vdots & \vdots & & \vdots & \vdots & 0 & \dots & 0 & 0 \\ \vdots & \vdots & & \vdots & \vdots & 0 & \dots & 0 & 0 \\ -q_{1,N-1} & -q_{1,N-2} & \dots & 0 & q_{N-1,N} & 0 & \dots & 0 & 0 \\ -q_{1,N} & -q_{2,N} & \dots & -q_{N-1,N} & 0 & q_{1,2} & \dots & q_{1,N-1} & q_{1,N} \\ 0 & 0 & \dots & 0 & -q_{1,2} & 0 & \dots & q_{2,N-1} & q_{2,N} \\ 0 & 0 & \dots & 0 & \vdots & \vdots & \dots & \vdots & \vdots \\ 0 & 0 & \dots & 0 & \vdots & \vdots & \dots & \vdots & \vdots \\ 0 & 0 & \dots & 0 & \vdots & \vdots & \dots & \vdots & \vdots \\ 0 & 0 & \dots & 0 & -q_{1,N-1} & -q_{1,N-2} & \dots & 0 & q_{N-1,N} \\ 0 & 0 & \dots & 0 & -q_{1,N} & -q_{2,N} & \dots & -q_{N-1,N} & q_{N,N} \end{bmatrix}$$

where  $\vec{U} = [U_1, U_2, \dots, U_{N-1}, U_N, U_{N+1}, \dots, U_{2N-2}, U_{2N-1}]^T$ . Note that the  $\hat{q}_{N,N}$  element is precisely zero because the contributions from  $q_{1,1}$  and  $q_{N,N}$  have equal magnitudes but opposite signs. These new matrices  $\hat{P}$  and  $\hat{Q}$  satisfy the summation-by-parts energy norm for precisely the same reasons as the original matrices  $P$  and  $Q$ . If the matrices are assembled in this manner, then the matrix  $\hat{P}$  is symmetric and the matrix  $\hat{Q}$  is skew symmetric except for the (1,1) and (2N-1, 2N-1) elements; these coefficients are again equal in magnitude but opposite in sign. Because the matrix  $\hat{P}$  can be decomposed into the summation of two matrices  $\hat{P}_1$  and  $\hat{P}_2$ , each of which is positive definite (one, but not both, could be positive semidefinite), the resulting matrix  $\hat{P}$  is positive definite. The new scheme is therefore stable because the summation-by-parts energy norm is satisfied. In practice, the scheme would be implemented as  $\hat{U}_t = \hat{P}^{-1} \hat{Q} \vec{U}$ . The inversion of the matrix  $\hat{P}$  could in general be quite complicated.

In short-hand notation, the new matrices  $\hat{P}$  and  $\hat{Q}$  can be written in terms of the original matrices  $P$  and  $Q$  as

$$\hat{P} = \begin{bmatrix} P & 0 \\ 0 & P \end{bmatrix}; \quad \hat{Q} = \frac{1}{\Delta} \begin{bmatrix} Q & 0 \\ 0 & Q \end{bmatrix}$$

This nomenclature is not precisely correct because the new matrix  $\hat{P}$  is  $(2N - 1 \times 2N - 1)$ , and the original  $P$  is  $(N \times N)$ . More precisely, the last row of the first matrix  $P$  and the first row of the second matrix  $P$  lie on the same row of the new matrix  $\hat{P}$ , with the inevitable intersection of matrices at the point  $\hat{p}_{N,N}$ . For the purposes of this work, this nomenclature will not cause any ambiguities.

Thus far in the derivation, we have assumed that the grid spacing in the first subdomain was the same as that in the second domain. In general, this assumption is not necessary, which we will demonstrate. Suppose that the first interval is discretized with a grid spacing  $\Delta_1$  and the second with a spacing  $\Delta_2$ . The resulting semidiscretizations would be  $P \vec{U}_t = \frac{1}{\Delta_1} Q \vec{U}$  and  $P \vec{U}_t = \frac{1}{\Delta_2} Q \vec{U}$ , respectively. Each respective discretization is multiplied by the appropriate grid spacing to yield  $\Delta_1 P \vec{U}_t = Q \vec{U}$  and  $\Delta_2 P \vec{U}_t = Q \vec{U}$ , respectively. The two subintervals are combined into one to yield the matrices  $\hat{P}$  and  $\hat{Q}$  of the form

$$\hat{P} = \begin{bmatrix} \Delta_1 P & 0 \\ 0 & \Delta_2 P \end{bmatrix}; \quad \hat{Q} = \begin{bmatrix} Q & 0 \\ 0 & Q \end{bmatrix}$$

The stability of the resulting scheme is guaranteed by the summation-by-parts energy norm for any arbitrary spacing discontinuity. In practice, the scheme would be implemented as  $\hat{U}_t = \hat{P}^{-1} \hat{Q} \hat{U}$ . The inversion of the matrix  $\hat{P}$  could in general be quite complicated. All information that pertains to the discontinuity in spacing is incorporated into the  $\hat{P}$  matrix.

This procedure of appending new subintervals onto an already existing method can be repeated recursively as many times as desired. In fact, even two dissimilar methods (each of which satisfies the summation-by-parts energy norm) can be appended to one another on any arbitrary grid-spacing interval. One constraint which the resulting cyclo-difference schemes must satisfy, is that the total number of grid points must be of the form  $N_t = M(N - 1) + 1$ , where  $N_t$  is the total number of points and  $M$  is the number of subintervals that are used. The procedure for grid refinement, therefore, involves an increase in the number of subintervals  $M$  in the solution.

## HIGH-ORDER CYCLO-DIFFERENCE SCHEMES

### Second Order

We now present a variety of cyclo-difference schemes of various order and width. In this work, we

will concentrate on schemes with uniform grid spacing within each subelement (but not necessarily the same from element to element). The first scheme of practical interest is the second-order scheme defined on a subelement of three grid points. The scheme represents the optimal second-order scheme on three uniformly spaced grid points and, in matrix notation, is given by

$$A^* = \begin{bmatrix} -3/2 & 2 & -1/2 \\ -1/2 & 0 & 1/2 \\ 1/2 & -2 & 3/2 \end{bmatrix}$$

It is readily shown that  $A^* = P^{-1}Q$ , where

$$P = \begin{bmatrix} 1/4 & 0 & 0 \\ 0 & 1 & 0 \\ 0 & 0 & 1/4 \end{bmatrix}; \quad Q = \begin{bmatrix} -3/8 & 1/2 & -1/8 \\ -1/2 & 0 & 1/2 \\ 1/8 & -1/2 & 3/8 \end{bmatrix}$$

This scheme is extended to five grid points to yield  $\hat{P}$  and  $\hat{Q}$  of the form

$$\hat{P} = \begin{bmatrix} 1/4 & 0 & 0 & 0 & 0 \\ 0 & 1 & 0 & 0 & 0 \\ 0 & 0 & 1/2 & 0 & 0 \\ 0 & 0 & 0 & 1 & 0 \\ 0 & 0 & 0 & 0 & 1/4 \end{bmatrix}; \quad \hat{Q} = \begin{bmatrix} -3/8 & 1/2 & -1/8 & 0 & 0 \\ -1/2 & 0 & 1/2 & 0 & 0 \\ 1/8 & -1/2 & 0 & 1/2 & -1/8 \\ 0 & 0 & -1/2 & 0 & 1/2 \\ 0 & 0 & 1/8 & -1/2 & 3/8 \end{bmatrix}$$

Because of the diagonal nature of the matrix  $\hat{P}$ ,  $\hat{P}^{-1}$  is easily found; the resulting numerical scheme is

$$\hat{A}^* = \begin{bmatrix} -3/2 & 2 & -1/2 & 0 & 0 \\ -1/2 & 0 & 1/2 & 0 & 0 \\ 1/4 & -1 & 0 & 1 & -1/4 \\ 0 & 0 & -1/2 & 0 & 1/2 \\ 0 & 0 & 1/2 & -2 & 3/2 \end{bmatrix}$$

The procedure is extended recursively to an arbitrary number of subelements to yield a cyclo-difference scheme of the form

$$\hat{A}^* = \begin{bmatrix} -3/2 & 2 & -1/2 & 0 & 0 & 0 & 0 & 0 & 0 & 0 & 0 & 0 & 0 \\ -1/2 & 0 & 1/2 & 0 & 0 & 0 & 0 & 0 & 0 & 0 & 0 & 0 & 0 \\ 1/4 & -1 & 0 & 1 & -1/4 & 0 & 0 & 0 & 0 & 0 & 0 & 0 & 0 \\ 0 & 0 & -1/2 & 0 & 1/2 & 0 & 0 & 0 & 0 & 0 & 0 & 0 & 0 \\ 0 & 0 & 1/4 & -1 & 0 & 1 & -1/4 & 0 & 0 & 0 & 0 & 0 & 0 \\ 0 & 0 & 0 & 0 & . & . & . & 0 & 0 & 0 & 0 & 0 & 0 \\ 0 & 0 & 0 & 0 & 0 & . & . & . & 0 & 0 & 0 & 0 & 0 \\ 0 & 0 & 0 & 0 & 0 & 0 & . & . & . & 0 & 0 & 0 & 0 \\ 0 & 0 & 0 & 0 & 0 & 0 & 1/4 & -1 & 0 & 1 & -1/4 & 0 & 0 \\ 0 & 0 & 0 & 0 & 0 & 0 & 0 & 0 & -1/2 & 0 & 1/2 & 0 & 0 \\ 0 & 0 & 0 & 0 & 0 & 0 & 0 & 0 & 1/4 & -1 & 0 & 1 & -1/4 \\ 0 & 0 & 0 & 0 & 0 & 0 & 0 & 0 & 0 & 0 & -1/2 & 0 & 1/2 \\ 0 & 0 & 0 & 0 & 0 & 0 & 0 & 0 & 0 & 0 & 1/2 & -2 & 3/2 \end{bmatrix}$$

This scheme is uniformly second-order accurate and satisfies the summation-by-parts energy norm. In addition, the scheme does not rely on auxiliary stencils at the boundaries. The operation count is  $\frac{3}{2}$  of the count for the conventional second-order scheme and, as will be shown later, behaves noticeably different.

In general, a closed-form expression for  $\hat{A}^*$  will not be available because the inverse of  $\hat{P}$  will not be known analytically. Therefore, a banded solver of width  $2N - 1$  (the number of points in each subelement) can be used on the matrix  $\hat{P}$  to efficiently invert the matrix. Although banded solvers are efficient in comparison with full solvers, they can not compete with explicit schemes in which no numerical inversion of the matrix  $\hat{P}$  must be performed. The previous example demonstrates that methods with a diagonal matrix  $P$  can be immediately inverted. By only concerning ourselves with those numerical methods that possess this property, we are being overly restrictive. In general, if  $P$  has a first and a last row that consists entirely of zeroes except for the diagonal element, then each subelement of the resulting matrix  $\hat{P}$  decouples and the inverse can be performed analytically. The resulting scheme has an explicit, not implicit, operation count and can compete with conventional finite-difference schemes of comparable spatial accuracy.

### Third Order

A uniformly third-order scheme can be generated with a minimum of four discrete points. The discretization matrix  $A^*$ , which is third order and occupies four points, can be represented as

$$A^* = \begin{bmatrix} -11/6 & 3 & -3/2 & 1/3 \\ -1/3 & -1/2 & 1 & -1/6 \\ 1/6 & -1 & 1/2 & 1/3 \\ -1/3 & 3/2 & -3 & 11/6 \end{bmatrix}$$

If  $A^*$  is decomposed into  $P^{-1}Q$ , the resulting relationships for  $P$  and  $Q$  are

$$P = \begin{bmatrix} r_3 & \frac{360r_3-11r_2+21r_1}{312} & \frac{-(54r_3-r_2+9r_1)}{78} & \frac{120r_3+5r_2+33r_1}{312} \\ \frac{360r_3-11r_2+21r_1}{312} & \frac{207r_3+7r_2+15r_1}{39} & \frac{-(72r_3+55r_2+51r_1)}{312} & \frac{-(54r_3-r_2+9r_1)}{78} \\ \frac{-(54r_3-r_2+9r_1)}{78} & \frac{-(72r_3+55r_2+51r_1)}{312} & \frac{207r_3+7r_2+15r_1}{39} & \frac{360r_3-11r_2+21r_1}{312} \\ \frac{120r_3+5r_2+33r_1}{312} & \frac{-(54r_3-r_2+9r_1)}{78} & \frac{360r_3-11r_2+21r_1}{312} & r_3 \end{bmatrix};$$

$$Q = \begin{bmatrix} \frac{-(288r_3-r_2+9r_1)}{117} & \frac{384r_3+3r_2+25r_1}{104} & \frac{-(24r_3+r_2+4r_1)}{13} & \frac{576r_3+37r_2+135r_1}{936} \\ \frac{-(384r_3+3r_2+25r_1)}{104} & 0 & \frac{576r_3+11r_2+57r_1}{104} & \frac{-(24r_3+r_2+4r_1)}{13} \\ \frac{24r_3+r_2+4r_1}{13} & \frac{-(576r_3+11r_2+57r_1)}{104} & 0 & \frac{384r_3+3r_2+25r_1}{104} \\ \frac{-(576r_3+37r_2+135r_1)}{936} & \frac{24r_3+r_2+4r_1}{13} & \frac{-(384r_3+3r_2+25r_1)}{104} & \frac{288r_3-r_2+9r_1}{117} \end{bmatrix}$$

The final criteria to be met is that the matrix  $P$  must be positive definite. Even if this scheme was stable for arbitrary  $r_1$ ,  $r_2$ , and  $r_3$ , the amount of work necessary to invert the matrix  $P$  would make the scheme prohibitively expensive. Therefore, the free parameters are used to decrease the bandwidth of the matrix  $P$ . If we set  $r_3 = 1$ ,  $r_2 = 9r_3$ , and  $r_1 = -5r_3$ , then  $P$  and  $Q$  result of the form

$$P = \begin{bmatrix} 1 & 1/2 & 0 & 0 \\ 1/2 & 5 & -1 & 0 \\ 0 & -1 & 5 & 1/2 \\ 0 & 0 & 1/2 & 1 \end{bmatrix}; \quad Q = \begin{bmatrix} -2 & 11/4 & -1 & 1/4 \\ (-11)/4 & 0 & 15/4 & -1 \\ 1 & (-15)/4 & 0 & 11/4 \\ (-1)/4 & 1 & (-11)/4 & 2 \end{bmatrix}$$

With Gershgorin's Theorem, the matrix  $P$  is shown to be positive definite. The original matrix satisfies the summation-by-parts energy norm and is stable for the hyperbolic system. Unfortunately, not enough free parameters exist in the decomposition to make  $P$  diagonal. The work involved in using a cyclo-difference scheme generated from  $P$  and  $Q$  would be seven multiplications and additions per node: four from the  $Q$  matrix and three from the inversion of the tridiagonal matrix  $\hat{P}$ . An operation count this high would not make the resulting scheme competitive with other third or higher order schemes.

To obtain high-order schemes in which  $P$  can be diagonalized, or at least decoupled from the other subelements, nonoptimal schemes must be used. Consider, for example, the family of uniformly third-order schemes that can be defined on five uniform points. Because each point allows a new degree of freedom, a wide variety of different schemes can be developed. Assuming that the following constraints are imposed: (1) uniform third-order accuracy exists from five points, (2) a  $P$  and  $Q$  exist that satisfy the summation-by-parts energy norm, and (3) a matrix  $P$  exists that has a first and last row composed entirely of zeros except the diagonal element. Matrices  $P$  and  $Q$  result of the form

$$P = \begin{bmatrix} 1 & 0 & 0 & 0 & 0 \\ 0 & \frac{-(13r_1-352)}{12} & \frac{7r_1-160}{6} & \frac{-(7r_1-160)}{12} & 0 \\ 0 & \frac{7r_1-160}{6} & \frac{-(25r_1-592)}{12} & \frac{7r_1-160}{6} & 0 \\ 0 & \frac{-(7r_1-160)}{12} & \frac{7r_1-160}{6} & \frac{-(13r_1-352)}{12} & 0 \\ 0 & 0 & 0 & 0 & 1 \end{bmatrix};$$

$$Q = \begin{bmatrix} \frac{3r_1-120}{32} & \frac{-(9r_1-256)}{24} & \frac{9r_1-208}{16} & \frac{-(3r_1-64)}{8} & \frac{9r_1-184}{96} \\ \frac{9r_1-256}{24} & 0 & 24-r_1 & \frac{3r_1-64}{3} & \frac{-(3r_1-64)}{8} \\ \frac{-(9r_1-208)}{16} & r_1-24 & 0 & 24-r_1 & \frac{9r_1-208}{8} \\ \frac{3r_1-64}{8} & \frac{-(3r_1-64)}{3} & r_1-24 & 0 & \frac{-(9r_1-256)}{16} \\ \frac{-(9r_1-184)}{96} & \frac{3r_1-64}{8} & \frac{-(9r_1-208)}{16} & \frac{9r_1-256}{24} & \frac{-(3r_1-120)}{32} \end{bmatrix}$$

The characteristic polynomial of the matrix  $P$  is

$$(\lambda - 1)^2 (2\lambda + r_1 - 32) [12\lambda^2 + (45r_1 - 1104)\lambda + 9r_1^2 - 560r_1 + 8192] = 0$$

for which the roots are  $\lambda = 1$ ,  $\frac{32-r_1}{2}$ , and  $\frac{-45r_1+1104}{24} \pm \frac{\sqrt{3}\sqrt{531r_1^2-24160r_1+275200}}{24}$ . For values of  $r_1 < \frac{280-8\sqrt{73}}{9}$ , all eigenvalues are positive, and the method is stable. The resulting matrix  $A^*$  can be written as

$$A^* = \begin{bmatrix} \frac{3r_1-120}{32} & \frac{-(9r_1-256)}{24} & \frac{9r_1-208}{16} & \frac{-(3r_1-64)}{8} & \frac{9r_1-184}{96} \\ \frac{-(r_1-48)}{6r_1-192} & \frac{-(7r_1-160)}{6r_1-192} & \frac{2r_1-48}{r_1-32} & \frac{-(5r_1-96)}{6r_1-192} & \frac{r_1-16}{6r_1-192} \\ \frac{1}{12} & \frac{-2}{3} & 0 & \frac{2}{3} & \frac{-1}{12} \\ \frac{-(r_1-16)}{6r_1-192} & \frac{5r_1-96}{6r_1-192} & \frac{-(2r_1-48)}{r_1-32} & \frac{7r_1-160}{6r_1-192} & \frac{r_1-48}{6r_1-192} \\ \frac{-(9r_1-184)}{96} & \frac{3r_1-64}{8} & \frac{-(9r_1-208)}{16} & \frac{9r_1-256}{24} & \frac{-(3r_1-120)}{32} \end{bmatrix}$$

Note that for a value of  $r_1 = \frac{160}{7}$  the resulting scheme is

$$P = \begin{bmatrix} 1 & 0 & 0 & 0 & 0 \\ 0 & 32/7 & 0 & 0 & 0 \\ 0 & 0 & 12/7 & 0 & 0 \\ 0 & 0 & 0 & 32/7 & 0 \\ 0 & 0 & 0 & 0 & 1 \end{bmatrix};$$

$$Q = \begin{bmatrix} (-45)/28 & 44/21 & (-1)/7 & (-4)/7 & 19/84 \\ (-44)/21 & 0 & 8/7 & 32/21 & (-4)/7 \\ 1/7 & (-8)/7 & 0 & 8/7 & (-1)/7 \\ 4/7 & (-32)/21 & (-8)/7 & 0 & 44/21 \\ (-19)/84 & 4/7 & 1/7 & (-44)/21 & 45/28 \end{bmatrix};$$

$$A^* = \begin{bmatrix} (-45)/28 & 44/21 & (-1)/7 & (-4)/7 & 19/84 \\ (-11)/24 & 0 & 1/4 & 1/3 & (-1)/8 \\ 1/12 & (-2)/3 & 0 & 2/3 & (-1)/12 \\ 1/8 & (-1)/3 & (-1)/4 & 0 & 11/24 \\ (-19)/84 & 4/7 & 1/7 & (-44)/21 & 45/28 \end{bmatrix}$$

Other third-order subelements exist for a uniform grid, but require a larger stencil. Their operation count is necessarily larger than those already presented and will not be pursued in this work.

#### Fourth Order

The optimal fourth-order schemes defined on five grid points produce a subelement  $A^*$  that can be decomposed into  $P$  and  $Q$  of the form

$$P = \begin{bmatrix} 1 & 2/3 & 0 & 0 & 0 \\ 2/3 & 20/3 & (-10)/3 & 4/3 & 0 \\ 0 & (-10)/3 & 32/3 & (-10)/3 & 0 \\ 0 & 4/3 & (-10)/3 & 20/3 & 2/3 \\ 0 & 0 & 0 & 2/3 & 1 \end{bmatrix};$$

$$Q = \begin{bmatrix} (-9)/4 & 31/9 & -2 & 1 & (-7)/36 \\ (-31)/9 & 0 & 6 & (-32)/9 & 1 \\ 2 & -6 & 0 & 6 & -2 \\ -1 & 32/9 & -6 & 0 & 31/9 \\ 7/36 & -1 & 2 & (-31)/9 & 9/4 \end{bmatrix};$$

$$A^* = \begin{bmatrix} (-25)/12 & 4 & -3 & 4/3 & (-1)/4 \\ (-1)/4 & (-5)/6 & 3/2 & (-1)/2 & 1/12 \\ 1/12 & (-2)/3 & 0 & 2/3 & (-1)/12 \\ (-1)/12 & 1/2 & (-3)/2 & 5/6 & 1/4 \\ 1/4 & (-4)/3 & 3 & -4 & 25/12 \end{bmatrix}$$

Gershgorin's theorem can be used to prove that the matrix  $P$  is positive definite. The scheme satisfies all criteria of the summation-by-parts energy norm and is, therefore, stable for hyperbolic systems. Note that the resulting scheme is pentadiagonal in the matrix  $P$  and would require a banded solver in the cyclo-difference mode to invert. The operation count of just the  $\hat{P}$  matrix inversion would be  $5N$ , which is not competitive with other explicit formulations. As the order of accuracy increases with optimal formulations, the bandwidth of the matrix  $P$  will also increase, which makes these schemes impractical. In addition, for  $N$  sufficiently large, the resulting schemes are unstable and cannot be used.

A subelement of uniformly fourth-order schemes that is stable and explicit can be derived by considering six uniformly distributed discrete points. One additional degree of freedom from each point enables all of the constraints to be met. As with the third-order subelements, a matrix  $P$  that decouples is sought. Matrices  $P$  and  $Q$  that satisfy these constraints are

$$P = \begin{bmatrix} 1 & 0 & 0 & 0 & 0 & 0 \\ 0 & \frac{-(2797 r_1 - 40008700)}{2745420} & \frac{287 r_1 - 2348300}{183028} & \frac{-(249 r_1 - 1862000)}{183028} & \frac{287 r_1 - 2348300}{549084} & 0 \\ 0 & \frac{287 r_1 - 2348300}{183028} & \frac{-(2999 r_1 - 20919400)}{915140} & \frac{557 r_1 - 3154500}{183028} & \frac{-(249 r_1 - 1862000)}{183028} & 0 \\ 0 & \frac{-(249 r_1 - 1862000)}{183028} & \frac{557 r_1 - 3154500}{183028} & \frac{-(2999 r_1 - 20919400)}{915140} & \frac{287 r_1 - 2348300}{183028} & 0 \\ 0 & \frac{287 r_1 - 2348300}{549084} & \frac{-(249 r_1 - 1862000)}{183028} & \frac{287 r_1 - 2348300}{183028} & \frac{-(2797 r_1 - 40008700)}{2745420} & 0 \\ 0 & 0 & 0 & 0 & 0 & 1 \end{bmatrix}$$

$$Q = \begin{bmatrix} \frac{72 r_1 - 2655360}{1143925} & \frac{-(864 r_1 - 14247875)}{2745420} & \frac{864 r_1 - 7384325}{1372710} & \frac{-(288 r_1 - 1698825)}{457570} & \frac{432 r_1 - 1976275}{1372710} & \frac{-(864 r_1 - 3266195)}{1372710} \\ \frac{864 r_1 - 14247875}{2745420} & 0 & \frac{-(1464 r_1 - 11209525)}{1372710} & \frac{2028 r_1 - 6385925}{1372710} & \frac{-(952 r_1 - 2851075)}{915140} & \frac{432 r_1 - 1976275}{1372710} \\ \frac{-(864 r_1 - 7384325)}{1372710} & \frac{1464 r_1 - 11209525}{1372710} & 0 & \frac{-(882 r_1 - 2557325)}{686355} & \frac{2028 r_1 - 6385925}{1372710} & \frac{-(288 r_1 - 1698825)}{457570} \\ \frac{288 r_1 - 1698825}{457570} & \frac{-(2028 r_1 - 6385925)}{1372710} & \frac{882 r_1 - 2557325}{686355} & 0 & \frac{-(1464 r_1 - 11209525)}{1372710} & \frac{864 r_1 - 7384325}{1372710} \\ \frac{-(432 r_1 - 1976275)}{1372710} & \frac{952 r_1 - 2851075}{915140} & \frac{-(2028 r_1 - 6385925)}{1372710} & \frac{1464 r_1 - 11209525}{1372710} & 0 & \frac{-(864 r_1 - 14247875)}{2745420} \\ \frac{864 r_1 - 3266195}{1372710} & \frac{-(432 r_1 - 1976275)}{1372710} & \frac{288 r_1 - 1698825}{457570} & \frac{-(864 r_1 - 7384325)}{1372710} & \frac{864 r_1 - 14247875}{2745420} & \frac{-(72 r_1 - 2655360)}{1143925} \end{bmatrix}$$

The roots of the characteristic polynomial of the matrix  $P$  are  $\lambda = 1, \frac{-167 r_1 + 3642325}{457570} \pm \frac{5\sqrt{5}\sqrt{101 r_1^2 - 2874060 r_1 + 20964334625}}{457570}$ , and  $\frac{-5396 r_1 + 40456475}{1372710} \pm \frac{5\sqrt{1076752 r_1^2 - 13981396400 r_1 + 48389568578125}}{1372710}$ . For values of  $r_1 < \frac{3627973675}{183168} - \frac{125\sqrt{425258307391537}}{183168}$  (a numerical value of about 5733), all eigenvalues are positive, and the method is stable.

### Fifth Order

Optimal subelements of fifth-order accuracy are not pursued in this work. Instead, a uniformly fifth-order accurate scheme defined on seven evenly spaced points is derived. The matrices  $P$  and  $Q$  are defined by

$$P = \begin{bmatrix} 1 & 0 & 0 & 0 & 0 & 0 & 0 \\ 0 & \frac{1069 r_1 + 292170384}{25286258} & \frac{-(89 r_1 + 7400232)}{1053594} & \frac{863 r_1 + 44908416}{8428752} & \frac{-(863 r_1 + 44908416)}{12643128} & \frac{89 r_1 + 7400232}{4214376} & 0 \\ 0 & \frac{-(89 r_1 + 7400232)}{1053594} & \frac{2627 r_1 + 11311560}{12643128} & \frac{-(1111 r_1 - 41866272)}{4214376} & \frac{809 r_1 - 13279392}{4214376} & \frac{-(863 r_1 + 44908416)}{12643128} & 0 \\ 0 & \frac{863 r_1 + 44908416}{8428752} & \frac{-(1111 r_1 - 41866272)}{4214376} & \frac{1489 r_1 - 72846720}{4214376} & \frac{-(1111 r_1 - 41866272)}{4214376} & \frac{863 r_1 + 44908416}{8428752} & 0 \\ 0 & \frac{-(863 r_1 + 44908416)}{12643128} & \frac{809 r_1 - 13279392}{4214376} & \frac{-(1111 r_1 - 41866272)}{4214376} & \frac{2627 r_1 + 11311560}{12643128} & \frac{-(89 r_1 + 7400232)}{1053594} & 0 \\ 0 & \frac{89 r_1 + 7400232}{4214376} & \frac{-(863 r_1 + 44908416)}{12643128} & \frac{863 r_1 + 44908416}{8428752} & \frac{-(89 r_1 + 7400232)}{1053594} & \frac{1069 r_1 + 292170384}{25286258} & 0 \\ 0 & 0 & 0 & 0 & 0 & 0 & 1 \end{bmatrix}$$

$$Q = \begin{bmatrix} \frac{-(25 r_1 + 26938800)}{12643128} & \frac{125 r_1 + 43031322}{10535940} & \frac{-(125 r_1 + 11423502)}{4214376} \\ \frac{-(125 r_1 + 43031322)}{10535940} & 0 & \frac{1255 r_1 - 486936}{25286256} \\ \frac{125 r_1 + 11423502}{4214376} & \frac{-(1255 r_1 - 486936)}{25286256} & 0 \\ \frac{-(125 r_1 + 887562)}{3180782} & \frac{185 r_1 - 28229184}{2107188} & \frac{-(305 r_1 - 88569864)}{4214376} \\ \frac{125 r_1 - 4380408}{4214376} & \frac{-(715 r_1 - 127212408)}{8428752} & \frac{680 r_1 - 204436503}{6321564} \\ \frac{-(25 r_1 - 1508238)}{2107188} & \frac{1475 r_1 - 205934976}{31807820} & \frac{-(715 r_1 - 127212408)}{8428752} \\ \frac{125 r_1 - 9648378}{63215640} & \frac{-(25 r_1 - 1508238)}{2107188} & \frac{125 r_1 - 4380408}{4214376} \end{bmatrix}$$

$$\begin{bmatrix} \frac{125 r_1 + 887562}{3180782} & \frac{-(125 r_1 - 4380408)}{4214376} & \frac{25 r_1 - 1508238}{2107188} & \frac{-(125 r_1 - 9648378)}{63215640} \\ \frac{-(185 r_1 - 28229184)}{2107188} & \frac{715 r_1 - 127212408}{8428752} & \frac{-(1475 r_1 - 205934976)}{31807820} & \frac{25 r_1 - 1508238}{2107188} \\ \frac{305 r_1 - 88569864}{4214376} & \frac{-(680 r_1 - 204436503)}{6321564} & \frac{715 r_1 - 127212408}{8428752} & \frac{-(125 r_1 - 4380408)}{4214376} \\ \dots & 0 & \frac{305 r_1 - 88569864}{4214376} & \frac{-(185 r_1 - 28229184)}{2107188} \\ \frac{-(305 r_1 - 88569864)}{4214376} & 0 & \frac{1255 r_1 - 486936}{25286256} & \frac{-(125 r_1 + 11423502)}{4214376} \\ \frac{185 r_1 - 28229184}{2107188} & \frac{-(1255 r_1 - 486936)}{25286256} & 0 & \frac{125 r_1 + 43031322}{10535940} \\ \frac{-(125 r_1 + 887562)}{3180782} & \frac{125 r_1 + 11423502}{4214376} & \frac{-(125 r_1 + 43031322)}{10535940} & \frac{25 r_1 + 26938800}{12643128} \end{bmatrix}$$

The matrix  $P$  is positive definite for values of  $r_1 > 172357$  (determined numerically). This uniformly fifth-order scheme satisfies the summation-by-parts energy norm and can be used as the subelement for generating a cyclo-difference scheme. The resulting scheme will be explicit in nature because the matrix  $\hat{P}$  can be inverted analytically.

This basic procedure can be used to generate schemes of arbitrarily high order, although none with an accuracy of greater the fifth order was generated in this work.

## STABILITY OF THE CYCLO-DIFFERENCE SCHEMES

The summation-by-parts energy norm was used to develop the cyclo-difference schemes in a semidiscrete context. The theoretical CFL for various Runge-Kutta (R-K) schemes must still be determined. Because each point in a cyclo-difference scheme uses a different stencil, the use of Fourier techniques to obtain a CFL is not applicable. A numerically determined eigenvalue spectrum provides a practical means of obtaining the CFL of the various schemes.

A necessary condition for Lax stability of a semidiscretization is that the eigenvalues of the spatial discretization operator (scaled by  $\Delta t$ ), lie within  $O(\Delta t)$  of the stability region of the time integration formula as  $\Delta t \rightarrow 0$ . This condition allows for exponential growth of the solution in time, but at a rate that is independent of the grid density, which guarantees convergence as  $\Delta x \rightarrow 0$ . For time asymptotic stability, all eigenvalues of the spatial discretization operator (scaled by  $\Delta t$ ) should lie

within the stability region of the time integration formula for all  $\Delta t$ . This condition guarantees that the solution in time will remain bounded if the solution to the original governing equation is bounded. The determination the CFL of a discretization is thus reduced to solving for  $\Delta t$  such that the resulting stability region of the time integration formula encompasses all spatial eigenvalues.

Figure 1 shows the eigenvalue spectrum of the cyclo-difference schemes as determined from a numerical eigenvalue determination. For each case, the number of grid points is 61; this number satisfies the grid constraints for all cyclo-difference schemes presented thus far. Note that the structure of the spectrum is not continuous, but seems to cluster into specific portions of the complex plane as for conventional finite-difference techniques. (See reference [2].) In addition, this clustering becomes more pronounced as the order of accuracy increases.

Table I shows the CFLs of the various schemes determined from a numerical eigenvalue determination. In all cases, the grid used contained 61 points. Very little sensitivity to grid density was observed between 31 and 61 grid points. The four algorithms used in the study were : 1) cyc23, 2) cyc35, 3) cyc46, and 4) cyc57. The first number indicates the formal accuracy of the scheme; the last number is the number of grid points occupied by the subelement stencil. The cyclo-difference schemes are then generated by recursively appending the subelements. Note that each scheme can only run on a grid of  $M(N - 1) + 1$  points, where  $N$  is the element size and  $M$  is the number of elements.

(R-K)	CFL	CFL	CFL	CFL
Order	Cyc23	Cyc35	Cyc46	Cyc57
2nd	Unstable	Unstable	Unstable	Unstable
3rd	1.16	1.23	1.08	0.87
4th	1.89	2.01	1.77	1.42

Table I. CFL of cyclo-difference schemes determined from eigenvalue determination.

Note that in each spatial operator, the fourth-order R-K is more efficient (in terms of CPU time, rather than storage) than the third-order R-K to advance the solution in time.

Interestingly, equation (14) was obtained *without imposing the boundary conditions*. Reference [5] demonstrated that the method of imposing physical boundary conditions is important to the overall stability of the method. Two counter examples showed that the property of time asymptotic stability could not in general be guaranteed for discretizations that satisfy the summation-by-parts norm.

The underlying reason for growth in time is the effect of the boundary operator on the structure of the norm matrix  $P^{-1}$ . Recall the semidiscrete form of equation (1):  $U_t = P^{-1} Q$ . If the boundary

operator  $D$  is imposed, the semidiscrete form  $U_t = D P^{-1} Q$  results, for which  $D P^{-1}$  may not be a norm. In the scalar case, this result is not a concern if the matrix  $P$  is a restricted full norm (Strand [4]) or if  $D P^{-1} = P^{-1} D$ . A restricted full norm is defined when the diagonal is the only nonzero element in the first (or last) row and column of the matrix  $P$ . The cyclo-difference schemes satisfy precisely the definition of the restricted full norm and, therefore, are automatically stable for the scalar wave equation.

Unfortunately, even for cases where  $P$  is a restricted full norm, stability cannot be generalized to the case of a general hyperbolic system. The SAT method proposed in reference [5] can be used to guarantee stability for the hyperbolic system. The SAT method involves the indirect imposition of the boundary conditions, which is accomplished by adding a term to the derivative operator that is proportional to the difference between the discrete value  $U_N$  and the boundary term  $f(t)$ . Rather than directly satisfying the boundary condition by imposing  $U_N = f(t)$ , the SAT method solves a derivative equation throughout the entire domain including the boundary points.

## ORDER PROPERTIES OF CYCLO-DIFFERENCE SCHEMES

### Time Dependent

Several test problems (both steady and unsteady) are used to establish the accuracy of the cyclo-difference schemes. Because Taylor series analysis was used in all cases to derive the schemes of a particular order, these schemes are expected to behave to at least the order of the local truncation error. Consider the method-of-lines approximation to the scalar wave equation

$$\frac{\partial U}{\partial t} + \frac{\partial U}{\partial x} = 0 \quad -1 \leq x \leq 1, t \geq 0 \quad (16)$$

$$U(t, -1) = \sin 2\pi(-1 - t); \quad U(0, x) = \sin 2\pi x \quad -1 \leq x \leq 1, t \geq 0 \quad (17)$$

with the exact solutions given by

$$U(t, x) = \sin 2\pi(x - t), \quad -1 \leq x \leq 1, t \geq 0 \quad (18)$$

The spatial discretization is accomplished by the new cyclo-difference schemes of various order; time was advanced with a four-stage R-K time-advancement scheme (formal nonlinear accuracy of fourth order) with a CFL of 0.25 to a time level of 25. Further temporal refinement showed no improvement in the solution accuracy.

### Uniform Mesh

We begin with a discretization on a uniform mesh. Table II shows the results from a grid-refinement study performed with each algorithm.

Grid	$\log L_2$			
	Cyc23	Cyc35	Cyc46	Cyc57
16			-1.347	
17		-0.7378		
19				-1.530
21	-1.662	-0.6959	-1.740	
25		-1.625		-2.059
29		-2.066		
31	-2.083		-2.276	-2.760
33		-2.218		
37				-3.273
41		-2.587	-2.722	
61	-2.710	-3.521	-3.736	-4.620
81		-3.914	-4.249	
91			-4.455	-5.678
101		-4.248	-4.638	
121	-3.316	-4.547	-4.956	-6.435

Table II. Accuracy of new cyclo-difference schemes as function of grid density.

Once a scheme has achieved a certain minimum grid density it will exhibit an order property; by doubling the mesh, the error will decrease by a factor of  $2^k$ , where  $k$  is the order of the scheme. The slopes for each scheme, as determined between grid densities of 31 (37 for cyc57) and 121 points, were -2.05, -4.05, -4.45, and -6.10, respectively.

Note that the apparent accuracy of some of the cyclo-difference schemes is higher than the predicted local truncation error. This result is more apparent in the schemes with an odd order, namely the cyc35 and the cyc57. The cyc46 does not obtain an accuracy that is significantly greater than the theoretical accuracy. Borrowing from the finite-element terminology, this increased convergence rate shall be referred to as "superconvergence."

### Discontinuous Mesh

We noted earlier in the derivation of the underlying principles of cyclo-differencing that two subintervals of unequal spacing could be joined at an interface without destroying the accuracy or stability of the formulation. The discretization matrices  $\hat{P}$  and  $\hat{Q}$  were defined by

$$\hat{P} = \begin{bmatrix} \Delta_1 P & 0 \\ 0 & \Delta_2 P \end{bmatrix}; \quad \hat{Q} = \begin{bmatrix} Q & 0 \\ 0 & Q \end{bmatrix}$$

Table III(a) shows the results of a grid-refinement study for which the ratio of grid spacings between subintervals was not one ( $\frac{\Delta_1}{\Delta_2} \neq 1$ ). The model problem was that used in the previous test case

(equations (16) to (18)), and the spatial discretization was the cyc35 algorithm. Time advancement was as previously described. In each case, the spatial domain was divided into two regions, and one half of the total number of points was distributed uniformly throughout each domain. This gave rise to grid spacings  $\Delta_1$  and  $\Delta_2$  in each domain, respectively. Table III(a) shows the logarithm of the  $L_2$  error for each discretization as a function of grid density, for a variety of spacing ratios  $\rho = \frac{\Delta_1}{\Delta_2}$ . In all cases, the finest concentration of mesh points occurred at the outflow boundary.

Grid	$\log L_2$			
	$\rho = 1$	$\rho = 3/2$	$\rho = 3$	$\rho = 5$
41	-2.587	-2.469	-1.864	-1.849
81	-3.914	-3.715	-3.197	-3.123
121	-4.547	-4.521	-3.974	-3.915
161	-5.046	-5.052	-4.559	-4.315

Table III(a). Accuracy of cyc35-difference scheme for discontinuous mesh spacing as function of grid density.

The magnitude of the error increases as the mesh discontinuity increases. This is because of the increased effective grid density that results from clustering the mesh points near the outflow boundary. The scheme still behaves with a fourth-order accuracy on this problem. Note that the slope of error decay for the  $\rho = 5$  case is -3.96 between  $N = 81$  and  $N = 161$  and that the cyc35 scheme is still superconvergent.

Table III(b) shows a similar comparison with the other cyclo-difference algorithms; all cases were run with a grid ratio of  $\rho = 5$ .

Grid	$\log L_2$		
	cyc35	cyc46	cyc57
41	-1.849	-2.317	
61			-3.251
81	-3.123	-3.279	
97			-4.449
121	-3.915	-3.983	-5.004
161	-4.315	-4.476	

Table III(b). Accuracy of cyclo-difference schemes for discontinuous mesh spacing ( $\rho = 5$ ) as function of grid density.

The slope of the error decay in the cyc57 scheme between points 61 and 121 is -5.82. The odd-order schemes, even in this discontinuous case, appear to be superconvergent.

## Steady State

The second test problem is the solution of the flow through a supersonic nozzle. The governing equations are the quasi-one-dimensional Euler equations. For this problem, an exact steady-state solution exists and can be used to compare the accuracy of the new cyclo-difference methods. The governing equations are

$$\begin{aligned}
 \frac{\partial}{\partial t} (\rho A) + \frac{\partial}{\partial x} (\rho u A) &= 0 \\
 \frac{\partial}{\partial t} (\rho u A) + \frac{\partial}{\partial x} [(\rho u^2 + p) A] &= p \frac{\partial A}{\partial x} \\
 \frac{\partial}{\partial t} (\rho e_t A) + \frac{\partial}{\partial x} [(\rho e_t + p) u A] &= 0
 \end{aligned} \tag{19}$$

where  $A = A(x)$  and  $e_t = CvT + \frac{u^2}{2}$ . Boundary conditions are imposed on the inflow plane for all three equations, and  $A(x)$  is prescribed such that the flow remains supersonic throughout the entire domain. A four- and a five-stage R-K were used to time advance the solution to the steady state (machine precision of  $10^{-13}$ ). Residual smoothing was used to accelerate the convergence rate for the various schemes. Table IV shows a comparison of the  $L_2$  error that resulted from each of the four cyclo-difference schemes on various grids.

Grid		$\log L_2$		
	Cyc23	Cyc35	Cyc46	Cyc57
121	-4.122	-5.450	-6.410	-6.851
181	-4.474	-6.153	-7.178	-7.916
241	-4.723	-6.653	-7.703	-8.666

Table IV. Accuracy of Cyclo-difference schemes as function of grid density for one-dimensional nozzle flow.

Note that by doubling the mesh, an error decay is produced with a slope of -2.00, -4.00, -4.29, and -6.00, respectively. These slopes agree with those obtained in the time-dependent case for simple linear advection. Again we see that the odd-ordered schemes are superconvergent.

Note that conventional second-order methods (as well as higher order central methods) with suitable boundary conditions will not converge to steady state for this and many other practical flow problems. The residual decreases only one order and then remains at this point indefinitely. This

non convergence is because the interior scheme is entirely dispersive; thus, the only dissipation in the spatial scheme comes from the boundary closure terms, which generally are not sufficient to damp the odd-even (" $\pi$ " in Fourier space) mode that can develop under non-linear circumstances. Higher order damping is explicitly added to these central-difference schemes to ensure that a steady-state solution can be found. The cyclo-difference schemes, by virtue of their cellular construction, are stable for the  $\pi$  mode and can be used without additional damping. In practice, additional damping makes the scheme converge more rapidly as expected.

## CONCLUSIONS

A new methodology referred to as "cyclo-differencing" is presented for defining stable high-order finite-difference schemes. They are similar to spectral element techniques of some arbitrary order, and are ideally suited for implementation on parallel machines. Unlike spectral element techniques, their existence does not rely on orthogonal polynomials or nonuniform grids. In principle, they can be devised of any order accuracy, although only schemes of sixth-order accuracy are pursued in this work. These new techniques rely on the summation-by-parts energy norm to establish formal stability for the scalar hyperbolic case. In addition, if the newly devised SAT method for imposing boundary conditions is used in conjunction with cyclo-differencing, then the resulting numerical method is formally stable for the hyperbolic system.

The cyclo-difference techniques are similar to central-difference techniques in that they are stable for right- or left-running waves, with appropriate placement of the physical boundary conditions. A decided advantage is that no numerical boundary conditions are required near the walls. Thus, high order accuracy is assured throughout the entire domain. In addition, the cyclo-difference schemes can be patched together across arbitrary grid discontinuities, and still retain their accuracy and stability.

A series of test problems are used to demonstrate the efficacy of the cyclo-difference methodology. The scalar advection equation is used to show the formal stability and accuracy of the second- to fifth-order cyclo-difference schemes. For the odd-order cyclo-difference schemes, the property of superconvergence is observed; specifically, these schemes converge at a rate one order higher than their theoretical accuracy on both uniform and discontinuous grids. A one-dimensional nozzle problem is used to demonstrate the robustness of the cyclo-difference techniques. Steady-state solutions, consistent with the order property of the spatial operator, are obtained without the addition of artificial damping to the formulations. Finally, the viscous Burgers equation is solved to demonstrate the use of the cyclo-difference technique for a nonlinear parabolic problem. Again, robust and accurate solutions are obtained in all cases.

## APPENDIX A

### Viscous Stability

Assume  $P \frac{\partial U}{\partial x} = Q U$ , where  $P$  and  $Q$  are matrix operators and  $U$  is a vector of discrete values. The proof of stability for the cyclo-difference scheme developed in this work relies on very specific forms for the matrices  $P$  and  $Q$ . Specifically,  $P = P^T$  and is positive definite;  $Q = Q_{sym} + Q_{sk}$ , where the only nonzero elements of  $Q_{sk}$  are  $q_{0,0}$  and  $q_{N,N}$ , and  $q_{0,0} = -q_{N,N} = -\alpha$ ; ( $\alpha > 0$ ). This form of the derivative operator leads directly to a stable second derivative operator. We begin with a derivation of the continuous energy for the one-dimensional heat equation

$$\frac{\partial U}{\partial t} = \alpha_d \frac{\partial^2 U}{\partial x^2} \quad 0 \leq x \leq 1, t \geq 0$$

$$U(0, t) = f(t); \quad U(1, t) = g(t)$$

$$U(x, 0) = \psi(x) \quad 0 \leq x \leq 1 \quad (\text{A. 1})$$

Note that boundary conditions based on the derivatives at  $x = 0$  or  $x = 1$  could have been imposed. An energy (defined as  $\frac{1}{2} U^2$ ) is formed by multiplying equation (A. 1) by  $U$ . Integration over the domain results in

$$E_t(t) = \int_0^1 [-\alpha_d U \frac{\partial^2(U)}{\partial x^2}] dx \quad t \geq 0 \quad (\text{A. 2})$$

Integration by parts yields an expression of the form

$$E_t(t) = \alpha_d [U(1, t) U_x(1, t) - U(0, t) U_x(0, t)] - \int_0^1 \alpha_d (\frac{\partial U}{\partial x})^2 dx \quad t \geq 0 \quad (\text{A. 3})$$

The energy takes the form of a negative definite quantity plus the boundary data that involve the function and its derivatives at the boundaries.

If the second derivative in equation (A. 1) is formed by twice operating with the first derivative operator, the semidiscrete form of equation (A. 1) becomes

$$\frac{\partial U}{\partial t} = \alpha_d P^{-1} Q P^{-1} Q U \quad t \geq 0 \quad (\text{A. 4})$$

If  $P$  is symmetric ( $P = P^T$ ) and is positive definite, then  $P^{-1}$  is symmetric and positive definite. Similarly, because  $Q = Q_{sym} + Q_{sk}$ , we have  $Q = 2 Q_{sym} - Q^T$ . By operating on equation (A. 4) from the left by  $U^T P$  and using the relationships between  $Q$  and  $Q^T$ , we obtain

$$E_t(t) = \alpha_d [2 U^T Q_{sym}^T P^{-1} Q U - U^T Q^T P^{-1} Q U] \quad t \geq 0 \quad (\text{A. 5})$$

where  $E_t$  is the time rate of change of the discrete energy defined by  $E(t) = U^T P U$ . In defining  $V = Q U$ , the second term on the right side of equation (A. 5) is negative definite. Because of the sparseness of the matrix  $Q_{sym}^T$ , the first term reduces to  $\alpha [U(1) \frac{\partial U}{\partial x}(1) - U(0) \frac{\partial U}{\partial x}(0)]$  and equation (A. 5) becomes

$$E_t(t) = \alpha_d \left[ 2\alpha \left( U(1) \frac{\partial U}{\partial x}(1) - U(0) \frac{\partial U}{\partial x}(0) \right) - V^T P^{-1} V \right] \quad t \geq 0 \quad (\text{A. 6})$$

To within a positive constant, this expression for the discrete energy is identical to that obtained from the continuous case. Therefore, the discrete energy will behave like the continuous energy. However, note that this analysis is linear and does not guarantee stability in some problems of practical interest. For example, the same argument could have been used to demonstrate the stability of forming  $U_{2x}$  from two central-difference first derivatives. In fact, if  $U_{2x}$  is formed in this manner, no damping would result for the  $\pi$  mode in Fourier space, which ultimately would result in the growth of the odd-even mode in physical space.

The cyclo-difference schemes do not appear to be as susceptible to the odd-even mode instability as the conventional central-difference schemes because a different stencil is used at each point. For example, consider the cyc35 scheme with the parameter  $r1 = 16$ . The resulting subelement  $A^* = P^{-1} Q$  is

$$A^* = \begin{bmatrix} -9/4 & 14/3 & -4 & 2 & -5/12 \\ -1/3 & -1/2 & 1 & -1/6 & 0 \\ 1/12 & -2/3 & 0 & 2/3 & -1/12 \\ 0 & 1/6 & -1 & 1/2 & 1/3 \\ 5/12 & -2 & 4 & -14/3 & 9/4 \end{bmatrix}$$

By forming the viscous derivative by the sequential operation of the first derivative operator  $A_v = A^* A^*$ , we obtain

$$A_v = \begin{bmatrix} 3 & -9 & 10 & -5 & 1 \\ 1 & -2 & 1 & 0 & 0 \\ 0 & 1 & -2 & 1 & 0 \\ 0 & 0 & 1 & -2 & 1 \\ 1 & -5 & 10 & -9 & 3 \end{bmatrix}$$

The interior of this matrix is identical to the conventional second-order viscous derivative and is not susceptible to the odd-even mode. Truncation analysis shows the resulting viscous matrix to be uniformly second order.

To test the convergence rate of the viscous terms and the overall influence of the odd-even mode, the viscous Burgers equation is used. The equation is defined by  $U_t + (0.5 U^2)_x = \mu U_{xx}$ , with boundary conditions  $U(0, t) = U_0$  and  $U(1, t) = 0$ . The exact steady-state solution is given by

$$U(x) = U_0 \bar{U} \left[ \frac{1 - \exp \bar{U} Re (x - 1)}{1 + \exp \bar{U} Re (x - 1)} \right]$$

where  $Re = U_0/\mu$  and  $\bar{U}$  is the solution of the equation

$$\frac{\bar{U} - 1}{\bar{U} + 1} = \exp(-\bar{U} Re)$$

and can be used to determine the error on a particular grid for this problem.

Table A.I shows the results of a grid-refinement study on the viscous Burgers equation.

Grid	fourth	Cyc35	Cyc46	Cyc57
51	-2.009		-3.547	
53		-3.405		
55				-2.975
101	-3.408	-4.663	-4.496	
103				-4.719
201	-4.879	-5.882	-6.233	
205				-6.807
401	-6.369	-7.087	-7.561	
403				-8.596

Table A.I: Error from various cyclo-difference schemes on the steady-state Burgers equation.

The  $\log_{10}$  of the  $L_2$  error are plotted as a function of the grid density. The convergence rate for the fourth, Cyc35, Cyc46, and Cyc57 methods are 4.9, 4.0, 5.1, and 6.5, respectively, as determined between the 101 and 401 points. The viscosity was  $\mu = 0.04$  which results in  $Re = 25$ .

## APPENDIX B

### Periodic Stability

At least two cycles of the fundamental subelement are required to define a cyclo-difference scheme (which includes two boundaries and one patch). Schemes of greater grid density can be constructed by cyclically patching an arbitrary number of subelements together. The cyclo-difference schemes can be used, however, on a periodic domain. By construction, we will show how to generate a stable periodic scheme from any of the cyclo-difference schemes.

The periodic assumption is implemented by first requiring that grid points 1 and  $N$  are equivalent. Hence, the last row and column from the cyclo-difference scheme can be eliminated. (With this requirement, the minimum number of subelements required for the periodic case is three.) If points 1 and  $N$  are equivalent, then the stencils that require grid point  $N$  are “wrapped around” to point 1. Similarly, the stencil at point 1 is replaced with the interface stencil symmetrically relates points on either side of grid point 1. The resulting cyclo-difference stencil is now periodic, and each subelement is indistinguishable in terms of position. Unlike conventional central-difference schemes, the resulting stencil is not skew symmetric. The eigenvalues of the stencil are all on the imaginary axis because  $A_p = P_p^{-1} Q_p$ , and  $Q_p$  is entirely skew symmetric.

The periodic versions of the cyc23 and cyc35 schemes are presented to illustrate this procedure. The periodic cyc23 scheme with three subelements (seven points) and truncated to six points, can be written as

$$A_p = \begin{bmatrix} 0 & 1 & -1/4 & 0 & 1/4 & -1 \\ -1/2 & 0 & 1/2 & 0 & 0 & 0 \\ 1/4 & -1 & 0 & 1 & -1/4 & 0 \\ 0 & 0 & -1/2 & 0 & 1/2 & 0 \\ -1/4 & 0 & 1/4 & -1 & 0 & 1 \\ 1/2 & 0 & 0 & 0 & -1/2 & 0 \end{bmatrix}$$

The matrix  $A_p = P_p^{-1} Q_p$ , where  $P$  is the diagonal matrix characterized by  $[1/2, 1, 1/2, 1, 1/2, 1]$  on the main diagonal;  $Q_p$  is entirely skew symmetric. By definition, we know that a skew symmetric matrix has eigenvalues on the imaginary axis. The semidiscrete energy of the system defined by  $U^T P_p U$  will be unchanged for all time with this discretization.

A comparison of the eigenvalues for this discretization with those of the conventional second-order periodic central-difference stencil on six points is interesting. The characteristic polynomial for the matrix  $A_p$  is  $\lambda^2 (16 \lambda^4 + 51 \lambda^2 + 36) = 0$ , which results in the eigenvalues  $\lambda = 0$  and  $\lambda = \pm \sqrt{3/32} \sqrt{17 \pm \sqrt{33}}i$  for which the maximum eigenvalue is  $\pm 1.46024$ . The conventional periodic second-order scheme produces a characteristic polynomial  $\lambda^2 (4 \lambda^2 + 3)^2 = 0$  for which the maximum eigenvalue is  $\sqrt{3/4}i$ . These eigenvalues are distinctly different; the effective CFL will be smaller for the cyc23 than for the conventional second-order scheme.

For simplicity, the diagonal form of the cyc35 scheme ( $r1=160/7$ ) will be used to illustrate the periodic form of the operator. The subelement  $A_5$  takes the form

$$A_5 = \begin{bmatrix} -\frac{45}{28} & \frac{44}{21} & -1/7 & -4/7 & \frac{19}{84} \\ -\frac{11}{24} & 0 & 1/4 & 1/3 & -1/8 \\ 1/12 & -2/3 & 0 & 2/3 & -1/12 \\ 1/8 & -1/3 & -1/4 & 0 & \frac{11}{24} \\ -\frac{19}{84} & 4/7 & 1/7 & -\frac{44}{21} & \frac{43}{28} \end{bmatrix}$$

Three subelements are used, and the resulting scheme is reduced by one row and column, which yields a matrix  $A_p$  of the form

$$A_p = \begin{bmatrix} 0 & \frac{22}{21} & -1/14 & -2/7 & \frac{19}{168} & 0 & 0 & 0 & -\frac{19}{168} & 2/7 & 1/14 & -\frac{22}{21} \\ -\frac{11}{24} & 0 & 1/4 & 1/3 & -1/8 & 0 & 0 & 0 & 0 & 0 & 0 & 0 \\ 1/12 & -2/3 & 0 & 2/3 & -1/12 & 0 & 0 & 0 & 0 & 0 & 0 & 0 \\ 1/8 & -1/3 & -1/4 & 0 & \frac{11}{24} & 0 & 0 & 0 & 0 & 0 & 0 & 0 \\ -\frac{19}{168} & 2/7 & 1/14 & -\frac{22}{21} & 0 & \frac{22}{21} & -1/14 & -2/7 & \frac{19}{168} & 0 & 0 & 0 \\ 0 & 0 & 0 & 0 & -\frac{11}{24} & 0 & 1/4 & 1/3 & -1/8 & 0 & 0 & 0 \\ 0 & 0 & 0 & 0 & 1/12 & -2/3 & 0 & 2/3 & -1/12 & 0 & 0 & 0 \\ 0 & 0 & 0 & 0 & 1/8 & -1/3 & -1/4 & 0 & \frac{11}{24} & 0 & 0 & 0 \\ \frac{19}{168} & 0 & 0 & 0 & -\frac{19}{168} & 2/7 & 1/14 & -\frac{22}{21} & 0 & \frac{22}{21} & -1/14 & -2/7 \\ -1/8 & 0 & 0 & 0 & 0 & 0 & 0 & 0 & -\frac{11}{24} & 0 & 1/4 & 1/3 \\ -1/12 & 0 & 0 & 0 & 0 & 0 & 0 & 0 & 1/12 & -2/3 & 0 & 2/3 \\ \frac{11}{24} & 0 & 0 & 0 & 0 & 0 & 0 & 0 & 1/8 & -1/3 & -1/4 & 0 \end{bmatrix}$$

The matrix  $A_p = P_p^{-1} Q_p$ , where  $P$  is the diagonal matrix characterized by  $[2, 32/7, 12/7, 32/7, 2, 32/7, 12/7, 32/7, 2, 32/7, 12/7, 32/7]$  on the main diagonal and  $Q_p$  is entirely skew symmetric. The semidiscrete energy of the system defined by  $U^T P_p U$  will be unchanged for all time with this discretization and is, therefore, stable when advanced with a stable time-advancement scheme. The characteristic polynomial for the matrix  $A_p$  is  $x^2(x^2 + 2)(9408x^8 + 23545x^6 + 18219x^4 + 4302x^2 + 243) = 0$ . The roots of this polynomial are strictly imaginary and are bounded by the points  $\pm\sqrt{2}i$ . Because the cyc35 scheme exhibits superconvergence properties, it can be compared with the conventional periodic fourth-order central difference expression defined on twelve grid points. The characteristic polynomial for the central difference case is  $x^2(9x^2 + 16)(16x^2 + 27)(48x^2 + 49)(20736x^4 + 19296x^2 + 3721) = 0$ . All roots are imaginary and are bounded by the points  $\pm\frac{4}{3}i$ . Again, note that the cyc35 scheme has a slightly more restrictive CFL than the conventional central-difference method on twelve points.

## References

- [1] B. Gustafsson, The Convergence Rate for Difference Approximations to Mixed Initial Boundary Value Problems, *Math. Comp.* **29**, 130, 1975, pp. 396-406.

- [2] M.H. Carpenter, D. Gottlieb, and S. Abarbanel, The Stability of Numerical Boundary Treatments for Compact High-Order Finite-Difference Schemes, NASA Contractor Report 187628, ICASE Report No. 91-71, Sept. 1991. Accepted for publication in *JCP*.
- [3] H.-O. Kreiss, and G. Scherer, Finite element and finite difference methods for hyperbolic partial differential equations, *Mathematical Aspects of Finite Elements in Partial Differential Equations*, (Academic Press, New York, 1974).
- [4] B. Strand, Summation by Parts for Finite Difference Approximations for  $d/dx$ , Dept of Scientific Computing, Uppsala University, Uppsala, Sweden, Aug., 1991.
- [5] M.H. Carpenter, D. Gottlieb, and S. Abarbanel, Time-Stable Boundary Conditions for Finite Difference Schemes Solving Hyperbolic Systems: Methodology and Application to High Order Compact Schemes, NASA Contractor Report, ICASE Report No. 93-09, Feb. 1993. Submitted to *JCP*.
- [6] G.E. Karniadakis, and S.A. Orszag, Parallel Spectral Computations of Complex Engineering Flow, Chapter 9 in *SuperComputing in Engineering Analysis*, (H. Adeli, ed.), to appear.
- [7] M.C. Macaraeg, and C.L. Streett, Improvements in Spectral Collocation through a Multiple Domain Technique, *Appl Num Math*, Vol. 2, No. 95, 1986.

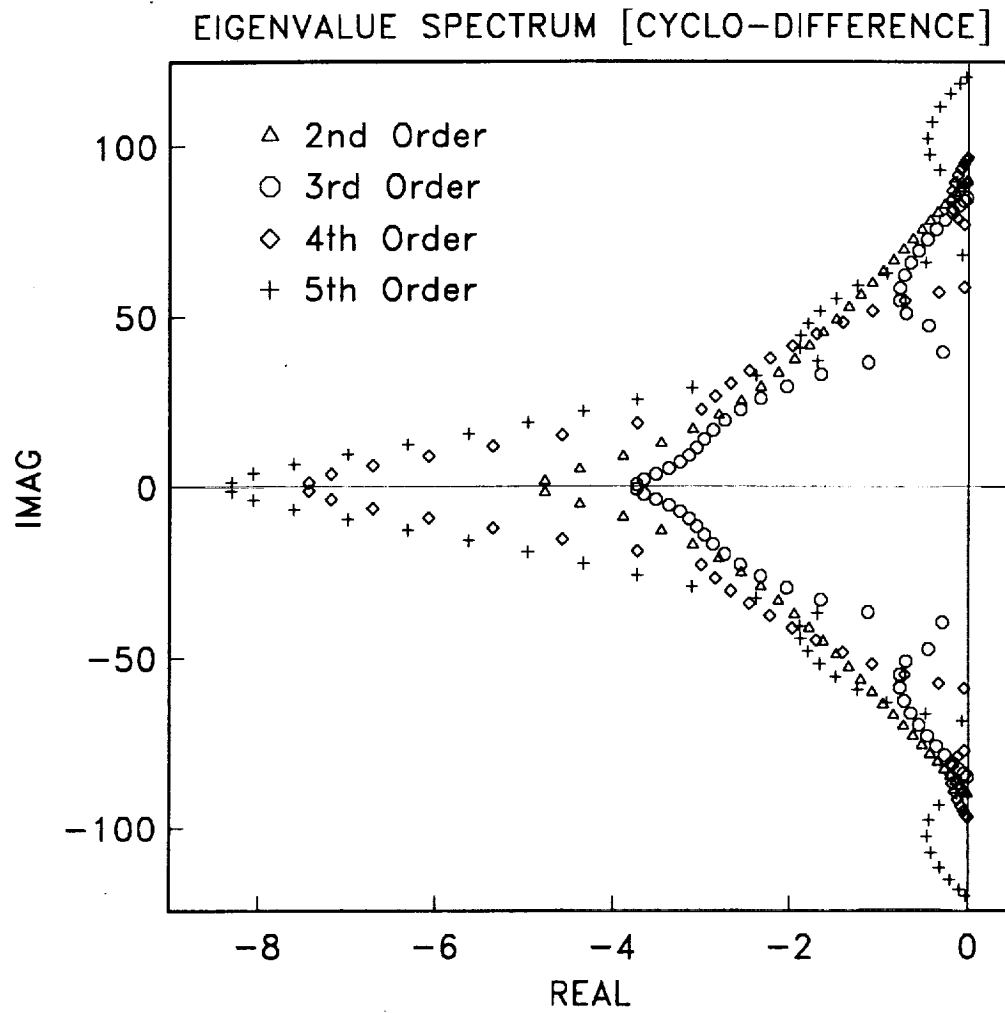


Figure 1. Eigenvalue spectra for second- to fifth-order cyclo-difference schemes with 61 gridpoints.

# REPORT DOCUMENTATION PAGE

Form Approved  
OMB No. 0704-0188

Public reporting burden for this collection of information is estimated to average 1 hour per response, including the time for reviewing instructions, searching existing data sources, gathering and maintaining the data needed, and completing and reviewing the collection of information. Send comments regarding this burden estimate or any other aspect of this collection of information, including suggestions for reducing this burden, to Washington Headquarters Services, Directorate for Information Operations and Reports, 1215 Jefferson Davis Highway, Suite 1204, Arlington, VA 22202-4302, and to the Office of Management and Budget, Paperwork Reduction Project (0704-0188), Washington, DC 20503.

<b>1. AGENCY USE ONLY (Leave blank)</b>	<b>2. REPORT DATE</b> March 1993	<b>3. REPORT TYPE AND DATES COVERED</b> Technical Memorandum	
<b>4. TITLE AND SUBTITLE</b> High-Order "Cyclo-Difference" Techniques: An Alternative to Finite Differences		<b>5. FUNDING NUMBERS</b> 505-70-62-06	
<b>6. AUTHOR(S)</b> Mark H. Carpenter John C. Otto			
<b>7. PERFORMING ORGANIZATION NAME(S) AND ADDRESS(ES)</b> NASA Langley Research Center Hampton, VA 23681-0001		<b>8. PERFORMING ORGANIZATION REPORT NUMBER</b>	
<b>9. SPONSORING/MONITORING AGENCY NAME(S) AND ADDRESS(ES)</b> National Aeronautics and Space Administration Washington, DC 20546-0001		<b>10. SPONSORING/MONITORING AGENCY REPORT NUMBER</b> NASA TM-107745	
<b>11. SUPPLEMENTARY NOTES</b>			
<b>12a. DISTRIBUTION/AVAILABILITY STATEMENT</b> Unclassified - Unlimited Subject Category 02		<b>12b. DISTRIBUTION CODE</b>	
<b>13. ABSTRACT (Maximum 200 words)</b>  The summation-by-parts energy norm is used to establish a new class of high-order finite-difference techniques referred to here as "cyclo-difference" techniques. These techniques are constructed cyclically from stable subelements, and require no numerical boundary conditions; when coupled with the simultaneous approximation term (SAT) boundary treatment, they are time asymptotically stable for an arbitrary hyperbolic system. These techniques are similar to spectral element techniques and are ideally suited for parallel implementation, but do not require special collocation points or orthogonal basis functions. The principal focus of this work is on methods of sixth-order formal accuracy or less; however, these methods could be extended in principle to any arbitrary order of accuracy.			
<b>14. SUBJECT TERMS</b> boundary condition stability, asymptotic stability, high-order finite-difference		<b>15. NUMBER OF PAGES</b> 28	
		<b>16. PRICE CODE</b> A03	
<b>17. SECURITY CLASSIFICATION OF REPORT</b> Unclassified	<b>18. SECURITY CLASSIFICATION OF THIS PAGE</b> Unclassified	<b>19. SECURITY CLASSIFICATION OF ABSTRACT</b> Unclassified	<b>20. LIMITATION OF ABSTRACT</b> UL